Journal of Applied Phycology (2026) 38:1465–1477
https://doi.org/10.1007/s10811-025-03776-7

RESEARCH

Pathogenicity of culturable bacteria isolated from an ice-ice-disease-infected *Kappaphycus striatus* green cultivar on the healthy brown cultivar

Hasriani Ayu Lestari[1] · Fahrurrozi Izzuddin[1] · Wahyu Purbiantoro[1] · Yanti Inneke Nababan[1] · Zaenal Arifin Siregar[1] · Hikmaturrohmi Hikmaturrohmi[2] · Eka Sunarwidhi Prasedya[2,3] · Michael Y. Roleda[1,4,5]

Received: 15 October 2025 / Revised: 7 December 2025 / Accepted: 25 December 2025 / Published online: 18 February 2026
© The Author(s) 2026

Abstract

The ice-ice disease (IID) impacting the commercially important eucheumatoid seaweed *Kappaphycus striatus* is characterized by thallus bleaching (whitening), softening, and subsequent disintegration of the affected tissue. The occurrence of IID is thought to be stress-related release of dissolve organic carbon exudates that are utilized as substrate for microbial growth. The presence of pathogenic bacteria can subsequently induce IID manifestations that can jeopardize crop health. In this study, we investigated the role of pathogenic bacteria isolated from diseased green cultivar of *K. striatus* in inducing IID symptoms in healthy non-axenic brown cultivar of the same species under controlled laboratory conditions. Healthy branches of *K. striatus* were exposed to four distinct bacterial strains: three isolated from the diseased *K. striatus* (*Vibrio brasiliensis* strain A8, *V. brasiliensis* strain B2 and *V. chemaguriensis* strain V1) and a positive control *Cytobacillus solani* strain-V2. Over a period of ten days, routine administration of each bacterium was conducted during the daily renewal of the filtered seawater medium. The occurrence of symptoms, i.e., typical of IID infection, was observed in samples subjected to additional bacterium but not under the control condition with natural microbiome. Our findings suggest that the presence of pathogenic bacteria, even under non-stressful laboratory conditions, can induce IID disease syndrome with various manifestations, including the development of wounds, abrasions, thallus bleaching, and fragmentation. The samples infected with the positive control *C. solani* strain-V2 exhibited the most severe bleaching at 80%, followed by *V. brasiliensis* strain-A8 at 60%, while *V. brasiliensis* strain-B2 and *V, chemaguriensis* strain-V1 both induced 50% thallus bleaching.

Keywords Bacteria · Bleaching · Cottonii seaweed · Eucheumatoid · *Vibrio* · *Cytobacillus solani*

Introduction

The commercial cultivation of the eucheumatoid *Kappaphycus* (primarily *K. alvarezii* and *K. striatus*) is predominantly dependent on the vegetative (clonal) propagation of a few haplotypes (Dumilag et al. 2023; Roleda et al. 2024; Gacura et al. 2026), leading to genetic uniformity among the cultivated populations. This homogeneity increases the susceptibility of *Kappaphycus* to disease outbreaks, particularly ice-ice disease (IID), which is characterized by thallus bleaching (whitening), softening, and subsequent disintegration of the affected tissues. IID is commonly associated with unfavorable alterations in environmental conditions, such as increased seawater temperature, decreased salinity due to precipitation, and other stressors. These changes jeopardize crop health, making seaweed more vulnerable to opportunistic pathogenic microorganisms (Ward et al. 2022).

✉ Hasriani Ayu Lestari
hasrianiayulestari93@gmail.com

✉ Michael Y. Roleda
myroleda@up.edu.ph

1 Research Center for Marine and Land Bioindustry, National Research and Innovation Agency, Lombok, Indonesia

2 Department of Biology, Faculty of Mathematics and Natural Sciences, University of Mataram, Mataram 83115, Indonesia

3 International Tropical Seaweed Center (ITSC), University of Mataram, Mataram 83115, Indonesia

4 Division of Food Production and Society, Norwegian Institute of Bioeconomy Research (NIBIO), P.O. Box 115, 1431 Ås, Norway

5 Algal Ecophysiology (AlgaE) Laboratory, College of Science, The Marine Science Institute, University of the Philippines, Diliman, 1101 Quezon City, Philippines

While the specific causative agents of IID remain inconclusive, previous studies have identified multiple microbial pathogens that contribute to disease symptoms. These include the bacteria *Vibrio sp*. P11 and *Cytophaga* sp. (Largo et al. 1995) and the marine fungi *Aspergillus ochraceus*, *A. terreus*, and *Phoma* sp. (Solis et al. 2010). However, under nutrient-enriched condition, eucheumatoids have shown to exhibit reduced susceptibility to IID (Luhan et al. 2015; Muyong and Tahiluddin 2024). These studies highlight the complex, pathobiotic nature of IID, which involves a combination of environmental stressors and microbial pathogens. However, most studies have focused on single bacterial inoculations at the beginning of the experiment with limited observation periods, typically lasting up to three weeks under batch culture conditions (Largo et al. 1995; Azizi et al. 2018). Similarly, investigations involving marine fungi used similar inoculation methods in nine-day observation period where disease symptoms progressively intensified from initial bleaching (starting day 3) to severe fragmentation across all infected thalli by day 9, demonstrating active disease progression without healing (Solis et al. 2010).

The current study aims to address these gaps by testing the pathogenicity of specific bacteria previously isolated from IID-infected green cultivar of *K. striatus* on healthy, non-axenic brown cultivar of the same species. This experiment involves the inoculation of four bacterial isolates: three *Vibrio* strains isolated from the diseased *K. striatus* (*V. brasiliensis* strain A8, *V. brasiliensis* strain B2 and *V. chemaguriensis* strain V1) and a positive control *Cytobacillus solani* strain-V2. Unlike the previous studies, we employ chronic exposure of healthy *K. striatus* to these bacterial pathogens during the daily medium renewal over a 10-day period to minimize the confounding effects of nutrient limitation. This design simulates persistent exposure of cultivated seaweed to marine microbes under farming conditions.

Materials & methods

Sample Collection

The commercially cultivated *Kappaphycus* species were collected from East Lombok, Indonesia where seaweed farming is thriving in Awang Bay (Fig. 1a, b). The IID-infected green cultivar of *Kappaphycus* sp. (L1KS1) was collected on April 25, 2024, in Farm A (8° 50' 57.3"S, 116° 24' 40.2"E) and the healthy brown cultivar (L1M1) was collected on August 3, 2024, in Farm B (8° 51' 05.2"S, 116° 24' 43.3"E). These farms are 248 m apart in the general vicinity of Batunampar, Jerowaru (Fig. 1c). The diseased sample green cultivar (Fig. 2a) was contained in a 50-mL Falcon tube, packed inside a styrofoam box with ice to keep cool and immediately transported to the laboratory for processing. Isolation of bacteria was described below. The healthy samples of brown cultivar (Fig. 2b) were brought to the outdoor hatchery facility of BRIN in Pemenang, allowed to acclimate for 2 days in a flow-through raceway before processing for the pathogenicity experiment (see methods described below). Both the green and brown *Kappaphycus* sp. cultivars were subjected to DNA barcoding (see methods described below) and sequence analyses showed that both are *K. striatus* (see results). Hereafter, the specimen used will be referred to as molecularly confirmed.

Kappaphycus species identification

Tissue of *Kappaphycus* sp. (3–5 cm) were kept in absolute ethanol until subsequent analyses. Genomic DNA was extracted with the DNeasy Mini Kit (Qiagen, Germany) following the manufacturer's instructions. The purity and concentration of DNA were evaluated with a Nanodrop spectrophotometer (Thermo Fisher Scientific, USA), where an absorbance ratio of ~1.8 was considered optimal for downstream molecular procedures.

Polymerase chain reaction (PCR) was carried out using a SensoQuest thermal cycler (Germany) to amplify the mitochondrial marker the cytochrome oxidase subunit 2–3 spacer (cox2-3s). PCR cycling conditions and primer sets followed the protocol of (Lim et al. 2014). Successful amplicons were purified and subjected to Sanger sequencing for nucleotide determination.

Sequence chromatograms were edited and assembled with ChromasPro v.2.1.10.1 (Technelysium, Australia). The resulting FASTA sequences were aligned with *Kappaphycus* and *Eucheuma* reference sequences from GenBank using ClustalX v.2.0 (Larkin et al. 2007). Multiple sequence alignments (MSAs) were then analyzed in IQ-TREE v.2.0.3 to select the best-fit Maximum Likelihood (ML) models based on the Bayesian Information Criterion (BIC). For cox2-3s, the HKY+F+I model was applied, with tree robustness assessed by 10000 ultrafast bootstrap replicates and 1000 approximate likelihood ratio tests (aLRT) (Nguyen et al. 2015).

Bacteria Isolation

The presumptive pathogenic bacteria associated with IID-infected green *K. striatus* cultivar was isolated upon arrival in the laboratory. After gently washing the tissue with sterilized seawater, 1 g was transferred into a 2-mL centrifuge tube containing sterile seawater and ground using a Micro Tissue Homogenizer (tissue grinder and pestle). Thereafter, 100 µL of serially diluted mixture samples were spread on R-2A agar (Himedia, India) and TCBS agar (Merck, Germany) plates and then incubated at 30 °C for 12 h.

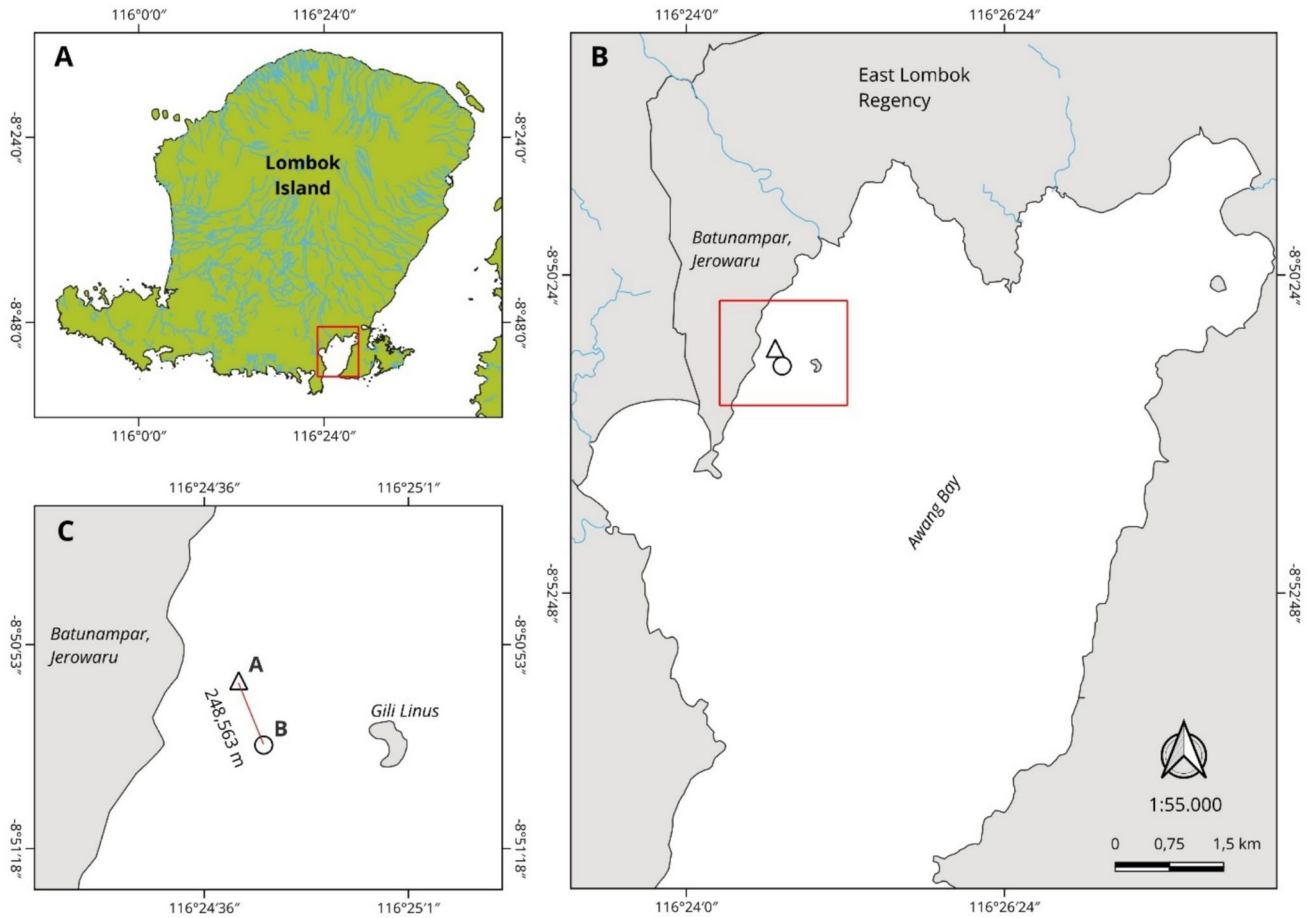


Fig. 1 Map of Lombok, Indonesia (**A**) where extensive seaweed farming is operating in Awang Bay (**B**). Diseased and healthy *Kappaphycus striatus* specimen were collected in Farm A [Δ] and B [○], respectively (**C**)

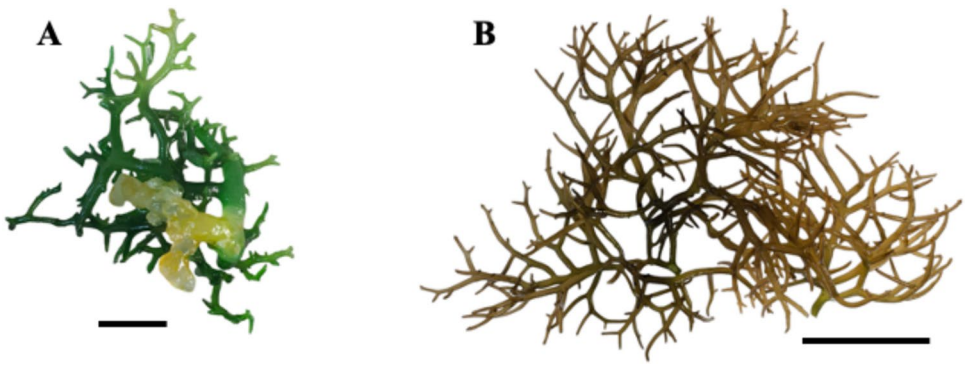


Fig. 2 Gross morphology of commercially cultivated *Kappaphycus striatus* as molecularly confirmed, collected in Fig. 1. Ice-ice-disease-infected green cultivar (**A**) and healthy brown cultivar (**B**) collected in Farms A and B, respectively. Scale bar = 5 cm

Bacteria molecular identification

Among more than 50 bacterial strains isolated from the diseased *K. striatus*, three strains were selected for pathogenicity experiment. The two strains, designated A8 and B2, were selected based on their capacity to degrade agar while the third strain (V1) was selected following preliminary species identification using CHROMagar Vibrio agar plates (CHROMagar, France), a selective medium that differentiates between species based on colony coloration. The observed cream-colored colonies indicated the presence of presumptive *Vibrio alginolyticus*, as previously reported (Chang et al. 2011). Additionally, V2 bacterium isolated from intestine of *Litopaneus vannamei*, was used as the positive control in the pathogenicity tests.

The taxonomic identity of the four bacteria was confirmed molecularly based on 16S rRNA gene sequencing. Genomic DNA of the two agar-degrading bacteria (A8 and B2), the presumptive *V. alginolyticus* (V1) and bacterium isolated from intestine of *L. vannamei* (V2) was extracted using the ZymoBIOMICS DNA Miniprep Kit (Zymo Research, USA), following the manufacturer's protocol., The 16S rRNA gene was amplified using universal primers 27 F (5'-AGAGTT TGATCMTGGCTCAG-3') and 1492R (5'-TACGGYTAC CTTGTTACGACTT-3'). Each 25 µL PCR reaction contained 12.5 µL of OneTaq 2x Master Mix (New England Biolabs, USA), 0.4 µL each of forward and reverse primers, 12 µL of sterile DNase- and RNA-free water, and 3 µL of DNA template. PCR products were verified by electrophoresis on a 1.2% (w/v) agarose gel in a 1x TBE buffer, and sequenced bidirectionally. The resulting sequences were matched against bacterial DNA sequences from the NCBI BLAST database (https://www.ncbi.nlm.nih.gov/) for taxonomic assignment. Sequences were aligned using ClustalW in MEGA 11. Phylogenetic trees were reconstructed using the Neighbor-Joining method, with evolutionary distances calculated by the Maximum Composite Likelihood model. Bootstrap analysis was performed with 1000 replicates, and branches supported by <50% bootstrap values collapsed in the consensus trees. For *Vibrio* isolates (V1, A8, and B2), *Aliivibrio fischeri*, *Photobacterium damselae* subsp. *damselae*, and *Grimontia hollisae* were used as a clade outgroup. For the V2 isolate, *Paenibacillus polymyxa* and *Staphylococcus aureus* were selected as outgroups.

Pathogenicity experimental design

From the healthy brown *K. striatus* cultivar, fifty apical branches weighing approximately 4–5 grams were excised from the clonal plants and allowed to heal wounds overnight in an outdoor aquarium. Thereafter, plants were further selected and acclimated for 2 days under laboratory conditions at 25 °C using filtered ambient seawater in 10-L glass aquarium. Seawater was passed through a sterile mixed cellulose ester (MCE) membrane filter with a pore size of 0.2 µm to obtain filtered ambient seawater. This process yields microbiologically sterile seawater while retaining the original chemical profile of the seawater. Selection criteria used were: (a) plants do not show visible spots (white, red, black); (b) no wounds and other visible tissue damage; and (c) no bleached tips. Branches were then meticulously cleaned of visible epiphytes using a magnifying glass lamp (Rectal magnifier with lamp, type 9WG23). During the pathogenicity experiment, plants were monitored as a holobiont.

To assess the pathogenic potential of the four bacterial isolates, a controlled infection assay was conducted using healthy, nonaxenic *K. striatus* thallus. The bacterial isolates previously barcoded were molecularly confirmed as *Vibrio brasiliensis* strain-1 (A8), *V. brasiliensis* strain-2 (B2), *V. alginolyticus* (V1)*, and Cytobacillus solani* (V2; see results section) hereafter designated as A8, B2, V1, and V2, respectively. For each bacterial treatment and the control, triplicates were prepared totaling to 15 experimental units.

The apical branches (4–5 g) were individually placed in 1-L glass jars filled with 0.20 µm-filtered ambient seawater. Each treatment group was subjected daily to 10^7 CFU mL^{-1} of the respective bacterial suspension over a 10-day exposure period. Fresh bacterial inocula were prepared daily and introduced into each experimental unit during routine exchange of seawater medium to simulate chronic exposure to potentially pathogenic bacteria.

The cultures were maintained in a temperature-controlled room set at 25 ± 1 °C under a 12:12 h light/dark cycle. Light was provided by two Philips Essential SmartBright LEDtubes (1200 mm, 16 W, 6500 K), delivering 100–120 µmol photons m^{-2} s^{-1} of photosynthetically active radiation (PAR) (Fig. 3). Fresh filtered seawater was replenished daily to ensure stable supply of macronutrients.

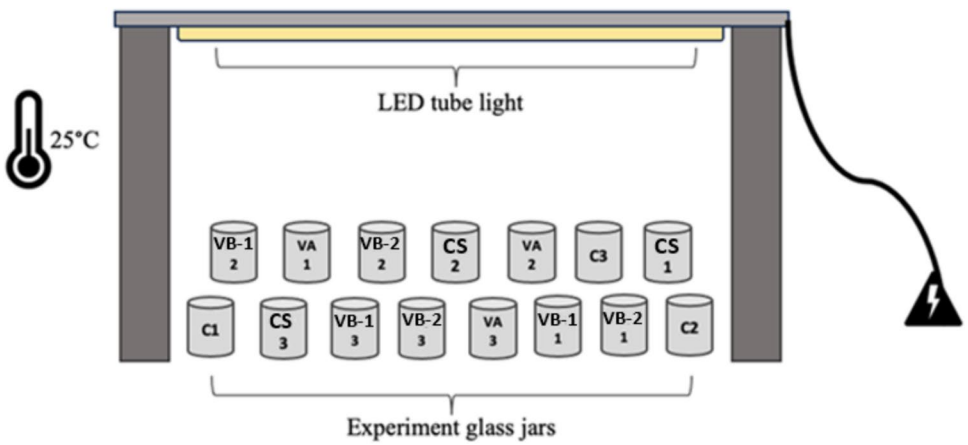


Fig. 3 Schematic diagram of the experimental setup with randomly arranged experimental units on a bank inside a temperature-controlled room at 25 °C, supplied with 12:12h light: dark photoperiod of 100–120 µmol m^{-2} s^{-1} PAR. The experimental units are routinely gently shaken and haphazardly rearranged 2–3× a day during the 10-day experimental duration

Pathogenesis and physiological response

The development of disease was monitored by conducting daily visual assessment of symptoms typical of IID syndrome such as depigmentation (bleaching), tissue softening, fragmentation, lesion formation, and structural disintegration of the thalli. The different manifestations were noted and scored as a percentage of change from photographs taken.

On day 10, i.e., at the end of the experiment, the pH of the culture medium in each jar was measured after the 24-hour batch culture period during the light phase (i.e., between 0900–1000h) using a portable digital pH meter (Adwa AD12; www.adwainstruments.com). The change in the medium's pH was used as a proxy for net metabolic activities of the holobiont. When the infected host tissue is decomposing, the higher microbial respiration can increase carbon dioxide and consequently lower pH (Narvarte et al. 2020). A lower pH may indicate the degree of infection severity.

Likewise, the relative growth rate was measured on day 10. The blotted wet weight (WW) of each sample was measured at the beginning (Day 0) and end (Day 10) of the experiment using a Sartorius analytical balance (BSA323S-CW). The percent relative growth rate (% RGR), expressed as % day^{-1}, was calculated using the following formula (Lin et al. 2010):

$$\%RGR = \left(\left(\frac{WW_f}{WW_i} \right)^{1/t} - 1 \right) \times 100$$

where WW_f and WW_i represent the final and initial wet weight of the thalli, respectively, and t is the duration of the experiment in days (t = 10). RGR was used as an indicator of algal growth performance and tissue integrity.

Statistical analysis

The assumptions of normality and homogeneity of variance of our data were not met. In this regard, the Kruskal–Wallis test (Kruskal and Wallis 1952) was employed as a non-parametric alternative to one-way ANOVA to evaluate differences among treatments, and defined as:

$$H = \frac{12}{n(n+1)} \sum_{i=1}^{k} \frac{R_i^2}{n_i} - 3(n+1)$$

where R_i is the sum of ranks in the i-th group, n_i is the sample size of group i, and n is the total number of observations. The null hypothesis states that the medians of all groups are equal (H_0), against the alternative hypothesis that at least one group median differs (H_1) (Vargha and Delaney 1998; Sherwani et al. 2021; Niedoba et al. 2023). When significant differences were identified, post hoc pairwise comparisons were conducted using Dunn's test with Bonferroni correction to adjust for multiple testing. All analyses were performed in R version 4.5.0 (R Core Team 2025), using the base stats package for the Kruskal–Wallis test and the FSA package for Dunn's post hoc analysis (Dino 2014; Ogle et al. 2015). The significance threshold was set at $\alpha = 0.05$.

Results

Kappaphycus species molecular identification

The cox2–cox3 sequence from L1KS1 (green cultivar; Fig. 4) produced top BLAST hits with 100% identity and 100% query coverage (E = 0.0; Max/Total Score = 654) to multiple accessions, including *Kappaphycus* sp. Aring-aring (KF687985.1) and several *Kappaphycus striatus* isolates (e.g., MZ170870.1, OL841130.1, MZ170853.1, MZ170867.1, OL841137.1). The perfect alignment across a 363–376 bp region indicates no mismatches between the query and subject sequences. The occurrence of both *Kappaphycus* sp. Aring-aring and *K. striatus* among the top matches reflects naming variations in GenBank records, where "Aring-aring" has been used in earlier submissions for specimens now recognized as *K. striatus*. The molecular evidence strongly supports the identification of L1KS1 as *K. striatus*. The complete identity across independent isolates deposited from different sampling campaigns confirms the robustness of this assignment. Unlike the L1M1 sequence (below, which showed 99.72% identity), L1KS1 matches with absolute identity, suggesting it is representative of a highly conserved haplotype within *K. striatus*.

The cox2–cox3 sequence from L1M1 (brown cultivar; Fig. 4) produced exclusively significant alignments to *K. striatus* (syn. *K. striatum*), with 99.72% identity, 100% query coverage, E = 1e-180, and Max/Total Score = 645 across multiple GenBank records (e.g., OL841127.1, OL841125.1, OL841120.1, JX624079.1, OL841122.1; alignment length ≈ 363 bp). No alternative *Kappaphycus* or *Eucheuma* taxa appeared among the top hits, indicating an unambiguous placement of L1M1 as *K. striatus*. The near-identical matches to diverse isolates (SLK, KRD, SIT, SCK series) from different submissions suggest very low intraspecific variation at this mitochondrial marker and reinforce the robustness of the assignment. The sequences were deposited to GenBank and are available under accession numbers PX441407 (L1KS1) and PX441406 (L1M1).

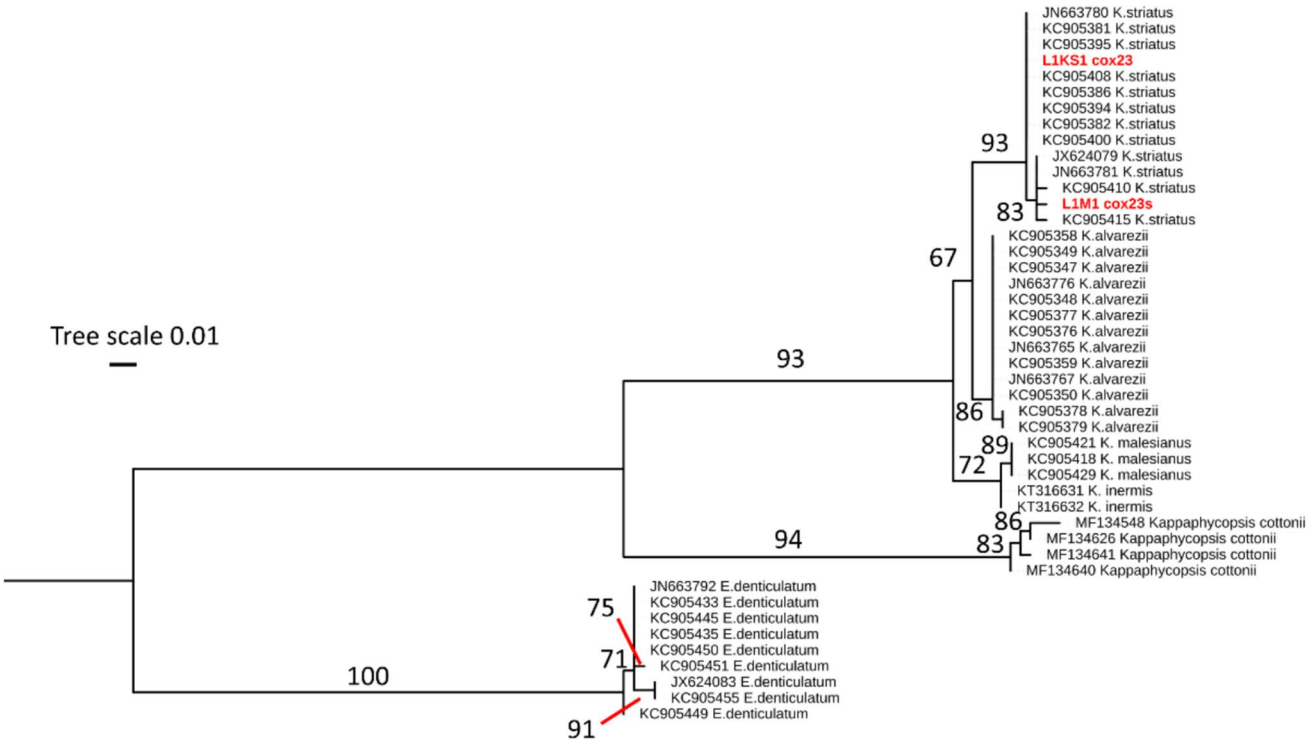


Fig. 4 Maximum likelihood phylogenetic tree of the cox2–cox3 intergenic spacer region showing the placement of L1KS1 (green cultivar) and L1M1 (brown cultivar), both highlighted in red, within the *Kappaphycus striatus* clade. Both sequences cluster tightly with reference accessions of *K. striatus* from GenBank, supported by high bootstrap values. The clade of *K. alvarezii* and other congeners (*K. malesianus*, *K. inermis*) are clearly separated, while *Eucheuma denticulatum* was used as the outgroup. Bootstrap values >50% are shown at the nodes, and the scale bar indicates substitutions per site

Bacterial identification based on 16S rRNA gene sequencing

The Neighbor-Joining phylogenetic tree based on 16S rRNA gene sequences (Fig. 5; Supplementary Data Fig. S1) showed that isolate V1 clustered with *Vibrio chemaguriensis* (bootstrap = 100%), whereas isolates A8 and B2 formed a clade with *V. brasiliensis* (bootstrap = 94%). Other reference species, including *V. parahaemolyticus*, *V. alginolyticus*, and *V. natriegens*, grouped separately with high support (89–99%). The tree was rooted with *Aliivibrio fischeri*, *Photobacterium damselae* subsp. *damselae*, and *Grimontia hollisae*, clearly distinguishing the *Vibrio* ingroup.

The phylogenetic tree of Bacillaceae (Fig. 6; Supplementary Data Fig. S2) placed isolate V2 within the *Cytobacillus* clade. V2 clustered closely with *Cytobacillus solani* and *C. praedii*, supported by high bootstrap values (100%). This clade was distinct from other Bacillaceae members such as *Bacillus mesophilum*, *Neobacillus bataviensis*, and *N. pocheonensis*. The tree was rooted with *Paenibacillus polymyxa* and *Staphylococcus aureus*, which formed a basal clade separate from *Cytobacillus* and *Neobacillus*.

Bacterial sequences were deposited in GenBank with the accession numbers PX458025, PX458046, PX458079, and PX458080 for *V. chemaguriensis* (V1), *V. brasiliensis* (A8), *V. brasiliensis* (B2), *Cytobacillus* sp. (V2) bacteria, respectively.

Pathogenesis and physiological response

Under the controlled laboratory conditions, growth rate of the control with natural microbial flora was minimal at 0.09 ± 0.04 % day^{-1} while growth of all treatments treated with additional bacteria were negative (ranging from −1.77% to −0.13%; Fig. 7). Growth rate was significantly higher in control and lowest in B2 (Kruskal-Wallis $\chi^2 = 10.63$, df = 4, $p = 0.031$; post hoc Dunn's test; Control > B2, adjusted $p = 0.014$). Growth rate under B2 was not significantly different to A8, V1 and V2 (B2 ≤ A8 ≤ V1 ≤ V2), while Control ≥ V2 ≥ V1 ≥ A8. The end pH at day 10 after 24 h incubation reflects similar trend to the growth rate where the lowest pH (7.8 ± 0.1) was measured under B2, suggesting higher bacterial heterotrophic activities impacting growth (Fig. 7). The control measured the highest pH at 8.3 ± 0.01. Despite the minimal increase in weight, the nonaxenic *K. striatus* under control (with its natural microbiome) maintained its healthy, firm, and dark pigmented appearance after 10 days (Fig. 8).

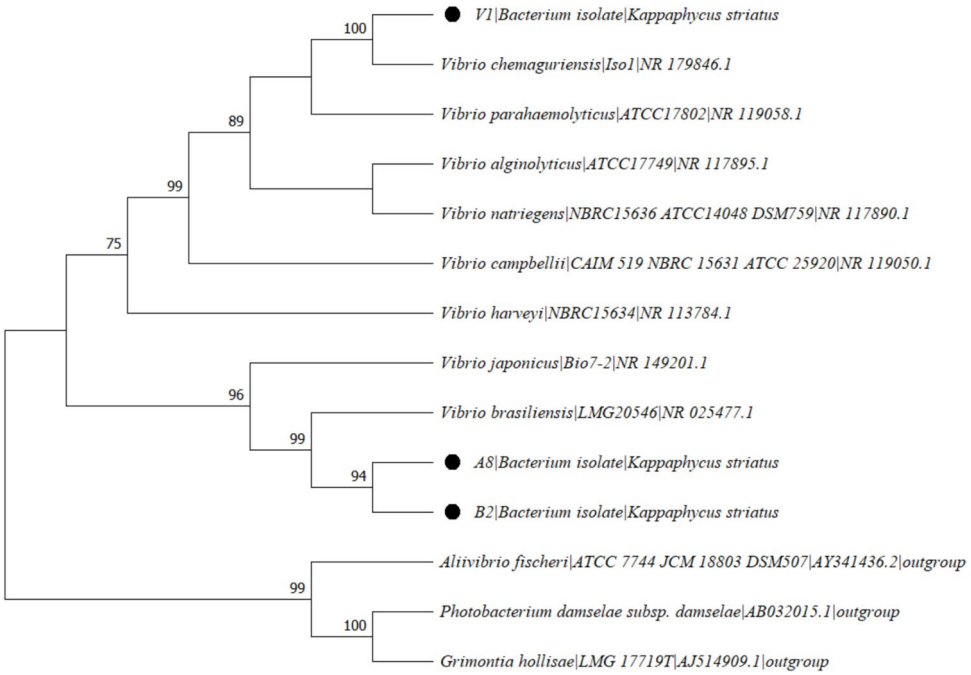


Fig. 5 Bootstrap consensus phylogenetic tree of *Vibrio* spp. (V1, A8, and B2) and related taxa constructed using the Neighbor-Joining method in MEGA 11. The bootstrap consensus tree was inferred from 1000 replicates; branches reproduced in less than 50% bootstrap replicates are collapsed. Bootstrap values below 70% are not shown. Evolutionary distances were computed using the Maximum Composite Likelihood method, based on 1555 nucleotide positions after pairwise deletion of ambiguous sites. The tree was rooted using *Aliivibrio fischeri, Photobacterium damselae* subsp. *damselae,* and *Grimontia hollisae* as a clade outgroup. Scale bar is not displayed due to software limitations; see Supplementary Figure S1 for the original tree with branch lengths

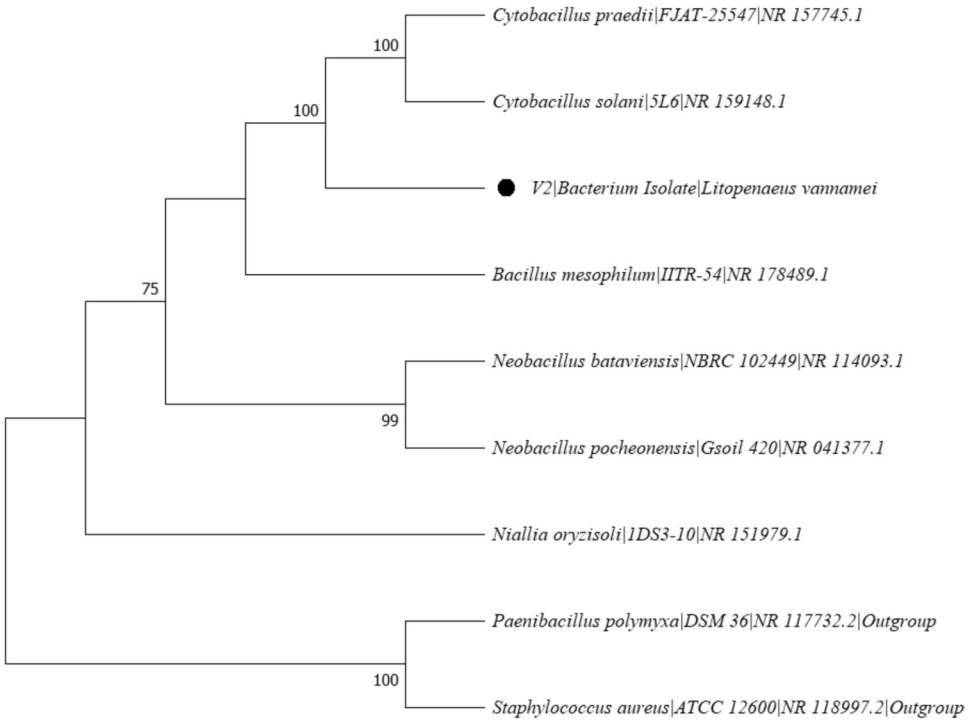


Fig. 6 Bootstrap consensus phylogenetic tree of *Cytobacillus* sp. V2 and related taxa constructed using the Neighbor-Joining method in MEGA 11. The bootstrap consensus tree was inferred from 1000 replicates; branches reproduced in less than 50% bootstrap replicates are collapsed. Bootstrap values below 70% are not shown. Evolutionary distances were computed using the Maximum Composite Likelihood method, based on 1564 nucleotide positions after pairwise deletion of ambiguous sites. The tree was rooted using *Paenibacillus polymyxa* and *Staphylococcus aureus* as a clade outgroup. Scale bar is not displayed due to software limitations; see Supplementary Figure S2 for the original tree with branch lengths

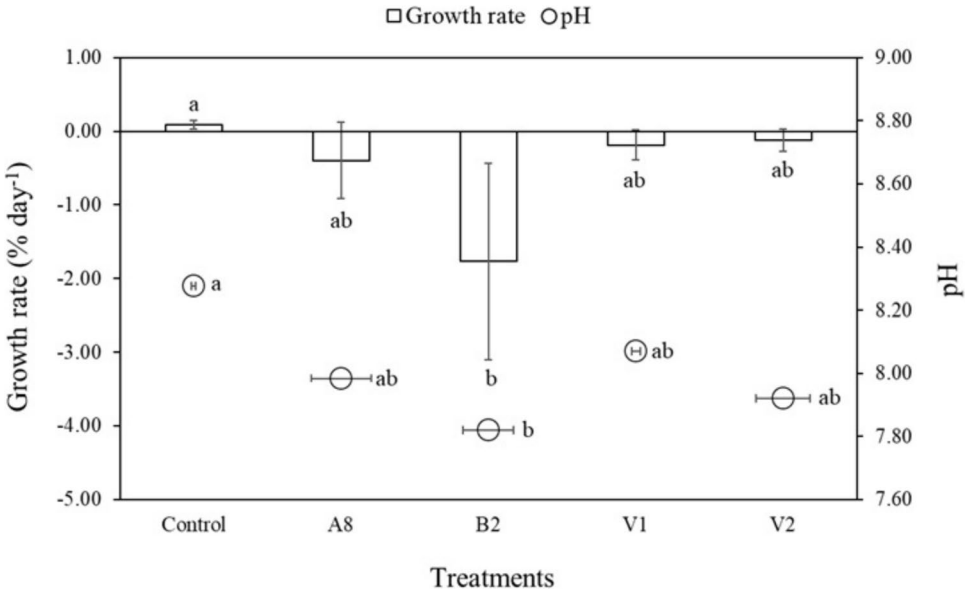


Fig. 7 Growth rate of *Kappaphycus striatus* after 10 days exposure to additional monospecific (A8, B2, V1 and V2) bacterial inoculum and corresponding end pH at day 10 after 24 h incubation (mean ±SE, $n = 3$). Non-parametric Kruskal-Wallis test and the FSA package for Dunn's post hoc analysis with significant threshold set at $\alpha = 0.05$ showed significant difference among treatments and different group(s) is designated by different letters

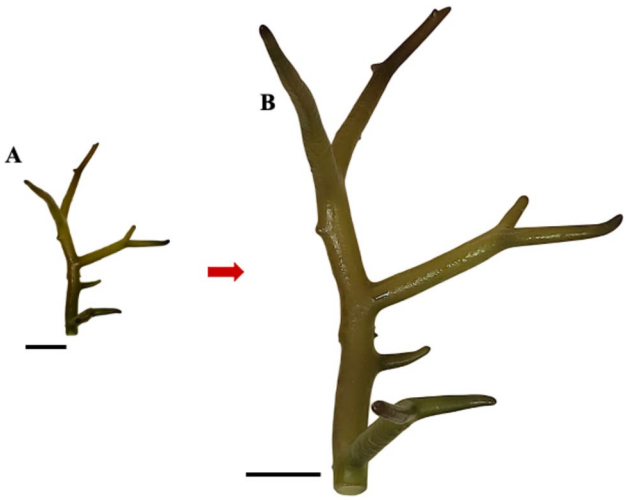


Fig. 8 Gross morphology of a representative *Kappaphycus striatus* at (**A**) the start of the experiment and (**B**) after the 10-day cultivation under control condition with natural microbiome showing darkly pigmented, healthy and unblemished thallus integrity. Scale bars: A = 5 cm, B = 3 cm

With the addition of A8, B2, V1 and V2 bacteria into the medium, all branches showed manifestation of disease (Figs. 9, 10, 11 and 12) such as: depigmentation and subsequent bleaching, apical meristematic tip erosion, abrasions, lesions, and softening of tissue and eventual fragmentation.

The initial manifestations of disease started already on day 3. On day 10, bleaching was most severe at 80% (including thallus depigmentation) in plants exposed to V2, followed by 60% in A8, and 50% in both B2 and V1. Pronounced secondary branch fragmentation after depigmentation that subsequently led to bleaching and softening of tissue was also observed in V2 treatment. Erosion of sharply pointed apical branches, i.e., highly meristematic, was observed in all treatments (Figs. 9, 10, 11 and 12). This tissue wasting phenomenon was observed after bleaching of the meristematic tips.

Discussion

This study is, to our knowledge, the first to show that experimentally manipulating the culture medium's microbial community by adding bacteria isolated from different origins, that subsequently affect the holobiont, can trigger manifestation of disease in *K. striatus* generally called ice-ice disease (IID) syndrome. The bacterial species composition and their relative density may control health and disease as different *Vibrio* species can be found in both healthy and diseased tissues of different eucheumatoid species (Aguilar RT and Roleda MY, unpublished data). On the other hand, the bacterium *C. solani* isolated from the gut of a shrimp also triggered IID. Under benign laboratory condition, which may be suboptimal, IID manifestation was solely triggered by the introduced bacteria. Whether the pathogenicity of a specific *Vibrio* species is dependent on its relative density in the holobiont warrants further study by checking if the same *Vibrio* species isolated from the diseased eucheumatoid are also present in the healthy plant or control.

Although abrasions and lesions are generally observed in primary and secondary branches which subsequently lead to depigmentation, softening of the tissue and bleaching, leading to thallus fragmentation, it is remarkable that the bacteria are effective in attacking the young apical tips that are highly meristematic. Among terrestrial plants, the

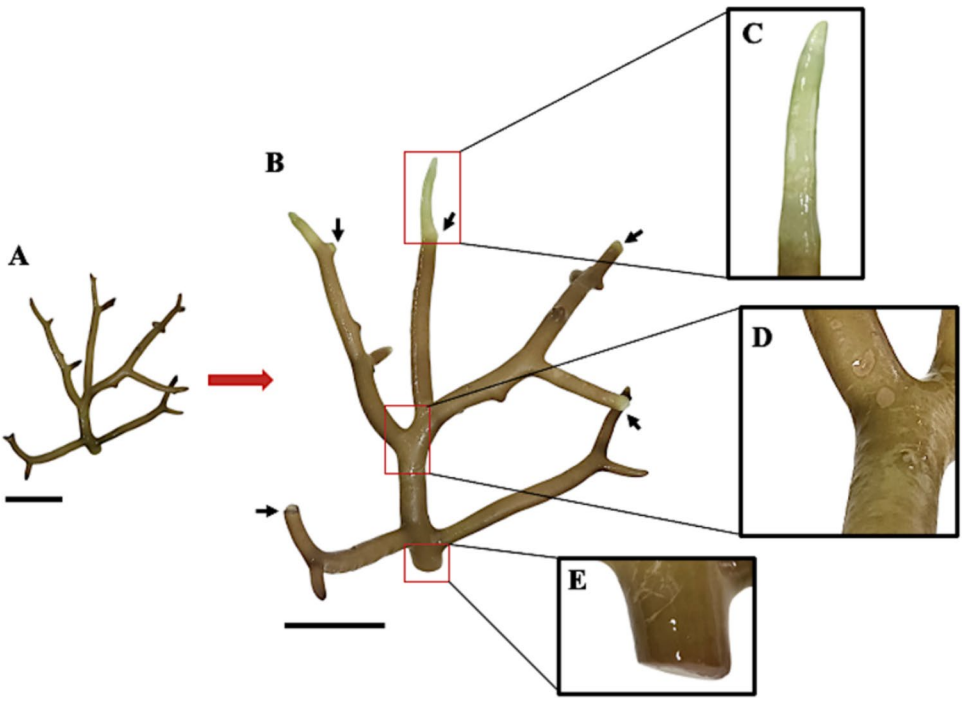


Fig. 9 Gross morphology of a representative *Kappaphycus striatus* at the (**A**) start of the experiment and (**B**) after the 10-day exposure to bacteria *Vibrio brasiliensis* strain-A8 isolated from the diseased green cultivar of the same species. Zoom out images (C–E) highlight disease manifestations such as bleaching (**C**; black arrows point to tissue erosion after bleaching of the pointed apical meristematic branches), depigmentation, abrasions, and softening of the primary and secondary branches (**D**), and abrasion and softening of the basal thallus segment (**E**). Scale bars = 5 cm (A) and 3 cm (B)

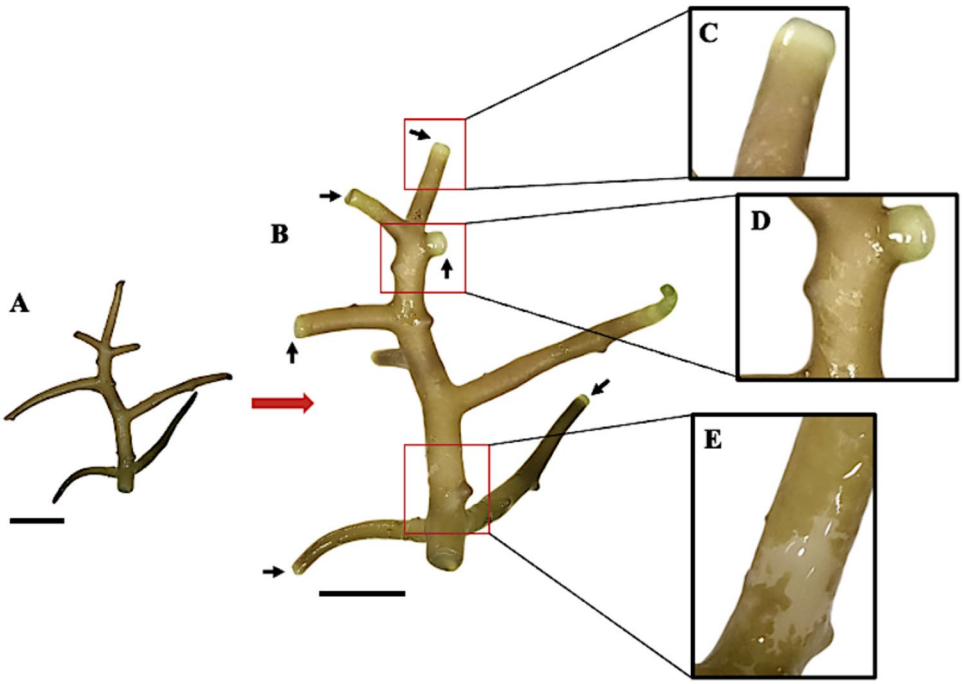


Fig. 10 Gross morphology of a representative *Kappaphycus striatus* at the (**A**) start of the experiment and (**B**) after the 10-day exposure to bacteria *Vibrio brasiliensis* strain-B2 isolated from the diseased green cultivar of the same species. Zoom out images (**C**–**E**) highlight disease manifestations such as tissue erosion after bleaching of the pointed apical meristematic branches (C and D; pointed by black arrows), depigmentation (D and E) and softening of the abraded primary branch (**E**). Scale bars = 5 cm (**A**) and 3 cm (**B**)

relationship between age and disease susceptibility has been investigated in many plant-pathogen systems, and older leaves/plants have been shown to exhibit increased resistance or reduced susceptibility to pathogens (Kus et al. 2002). Such age-related resistance (ARR) has not been explored among macroalgae.

The phylogeny confirmed that isolate V1 is affiliated with *V. chemaguriensis*, not *V. alginolyticus* as suggested by CHROMagar identification, underscoring the limitations of culture-based methods for closely related *Vibrio* species. Isolates A8 and B2 clustered with *V. brasiliensis*, indicating a close evolutionary relationship that may reflect shared ecological or pathogenic roles in IID. The selected outgroups (*A. fischeri*, *P. damselae*, *G. hollisae*) appropriately represent external Vibrionaceae lineages, ensuring robust rooting. Meanwhile, isolate V2 grouped with *Cytobacillus* spp.,

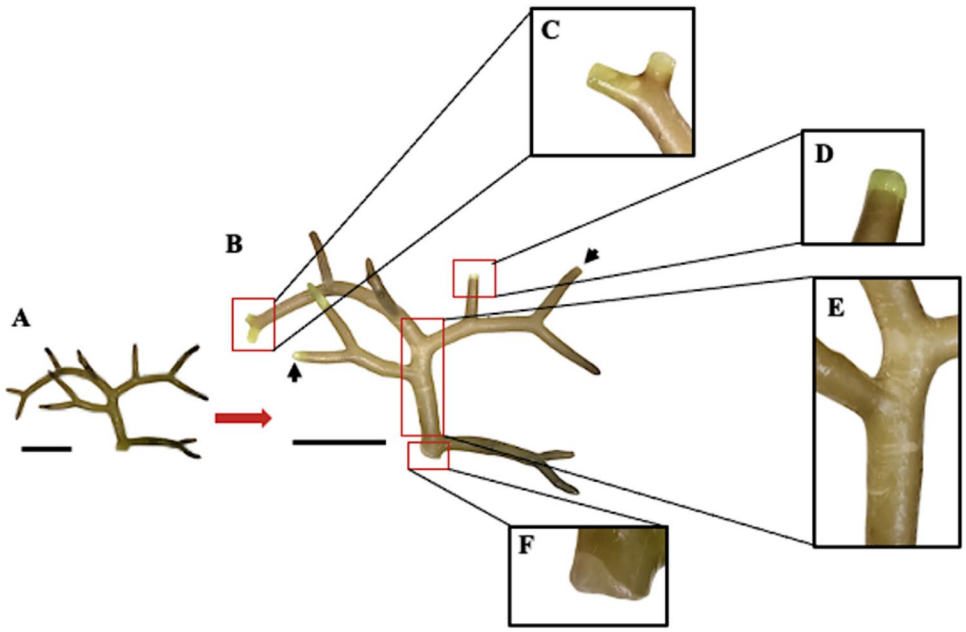


Fig. 11 Gross morphology of a representative *Kappaphycus striatus* at the (**A**) start of the experiment and (**B**) after the 10-day exposure to bacteria *Vibrio chemaguriensis* strain-V1 isolated from the diseased green cultivar of the same species. Zoom out images (C–F) highlight disease manifestations such as bleaching and tissue erosion of the sharply pointed apical meristematic branches (C and D; pointed by black arrows), depigmentation and abrasions on the primary and secondary axes (**E**) and softening of the basal thallus segment (**F**). Scale bars = 5 cm (A) and 3 cm (B)

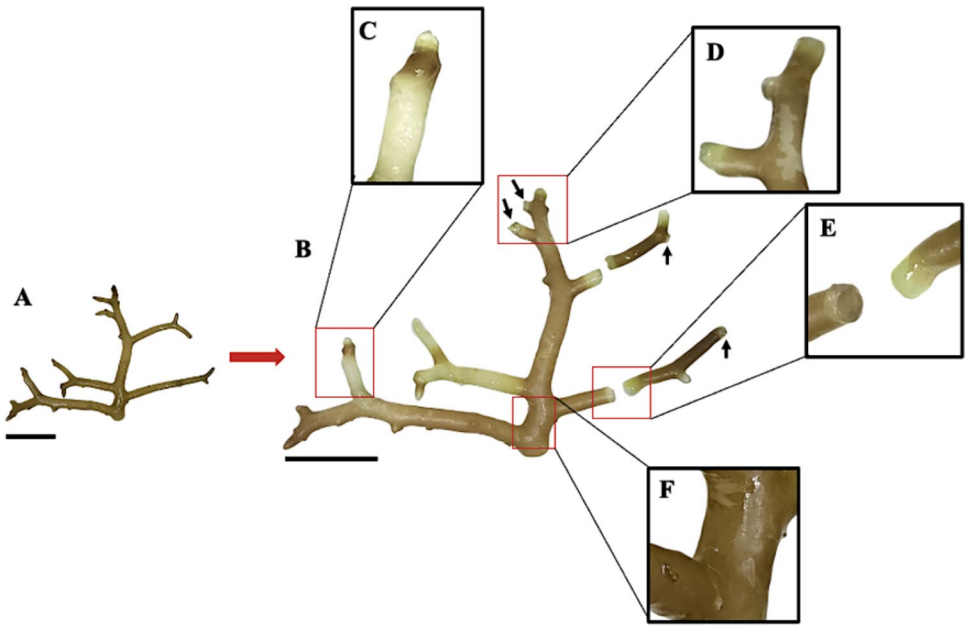


Fig. 12 Gross morphology of representative *Kappaphycus striatus* at the (**A**) start of the experiment and (**B**) after the 10-day exposure to positive control bacteria *Cytobacillus solani* strain-V2 isolated from the intestine of *Litopenaeus vannamei*. Zoom out images (**C**–**F**) highlight disease manifestations such as bleaching (C), tissue erosion of the sharply pointed apical meristematic tissue (**D**; pointed by black arrows), fragmentation of secondary branch after bleaching, softening and erosion of tissue (**E**), and abrasions on the primary branch. Scale bars = 5 cm (**A**) and 3 cm (**B**)

strongly supported by its proximity to *C. solani* and *C. praedii*. This confirms its placement outside *Bacillus*, consistent with recent taxonomic revisions of Bacillaceae. The use of *P. polymyxa* and *S. aureus* as outgroups provided clear tree orientation. Overall, 16S rRNA phylogeny provided higher taxonomic resolution than preliminary phenotypic identification, clarifying the affiliations of culturable bacteria associated with IID.

Our experiment showed that individual pathogenic bacterial strains induced symptoms that are different from the classic IID phenotype, e.g., diseased green *K. striatus* cultivar (Fig. 2A). This suggests that canonical IID syndrome manifestation may require a complex of stress factors and co-infecting microbes rather than a single pathogen. Indeed, Ward et al. (2022) emphasize that IID is a multifactorial syndrome with no single causal agent identified. For example, (Largo et al. 1995) isolated both a *Vibrio* sp. and a *Cytophaga*-related (Flavobacterium) strain from bleached *Kappaphycus* and showed that each could trigger premature whitening under stress. In our case, the atypical symptoms from single-bacterium inoculation imply that classic IID bleaching (and tissue softening) may arise from synergistic

interactions of multiple pathogenic bacteria and fungi under stress, whereas individual pathogen alone (i.e., in addition to the natural microbiome) may cause different disease manifestations (e.g., lesions and abrasions) or these are early warning signs and symptoms not commonly observed in the field due to monitoring limitations.

The severity of disease manifestations varied among clones exposed to the same bacteria. The clonal variation observed may be associated with genetic and/or physiological (and associated biochemistry, e.g., pigments) differences among clones of the same cultivar that can affect traits such as growth, biochemistry and resistance to disease (biotic) and abiotic stressors. The occurrence and accumulation of mutations among clones of the same cultivar also contribute to genetic variations. Thereafter, these mutations are reproduced unmodified in subsequent cuttings of the mutated clone. Due to the slow accumulation of mutations, old cultivars have a greater probability of consisting of several clones, differing by one or more mutations. The presumptive variations in our clones of brown *K. striatus* cultivars derived from several plants (i.e., bunches of farmed eucheumatoid) from a seaweed farm may have contributed to the differential susceptibility to and severity of the disease. Recently, Gacura and co-workers (2026) reported strain-specific susceptibility to IID among different *K. alvarezii* (novel strains and commercially cultivated haplotypes) cultivars. The prevalence of IID was also reported to be higher during dry compared to wet season (Tahiluddin and Terzi 2024). Among seaweed farmers in Tawi-Tawi, southern Philippines, they narrated that *K. striatus* are more susceptible to IID compared with *K. alvarezii* and *E. denticulatum* (Tahiluddin and Eldani-Tahiluddin 2024). This narrative could vary seasonally across different farm sites and may be subject to seaweed farmers' bias. A well-designed common garden experiment is necessary to test the relative susceptibility to IID among different eucheumatoid species. This is important because carrageenan yield and quality of IID-infected crops can be severely compromised (Mendoza et al. 2002). Higher levels of accessory pigments (phycobiliproteins) and polyphenols among brown cultivars may inhibit bacterial enzymatic activity or enhance host immune responses. Future research is needed to identify the specific pigments or secondary metabolites responsible for plant stress response.

Farm management strategies, e.g., biosecurity intervention, and application of biotechnological techniques can help minimize pest and disease occurrence and severity. Selection and use of robust cultivars is of prime importance. Biotechnological techniques may provide further protection to minimize crop failure due to pests and disease. For example, manipulation of the microbiome by introducing beneficial bacteria offer promise. A recent study showed that a *V. alginolyticus* probiotic strain can significantly reduce bleaching in farmed kelp (Ma et al. 2023). The same probiotic approaches may be researched and applied to protect eucheumatoid crops.

Rigorous implementation of seaweed farm biosecurity thorough cleaning of lines and equipment, early disease monitoring, etc., have been shown to dramatically cut IID incidence by ~60–75% (Kambey et al. 2021). In addition, diversifying or rotating species (e.g., co-culturing with non-susceptible seaweeds that inhibit pathogens) could suppress outbreak severity. For example, field studies in Hainan, China demonstrated that co-cultivating *Kappaphycus* with the more resistant *Eucheuma denticulatum* resulted in markedly lower IID incidence, highlighting the potential of polyculture to mitigate disease outbreaks (Pang et al. 2015). More recently, Pang et al. (2025) reported that in the co-cultivation of *Gracilariopsis lemaneiformis* and *Saccharina japonica*, a bacterial species (*V. alginolyticus*) previously considered beneficial to one host (*S. japonica*) was found to be pathogenic to the other (*G. lemaneiformis*), providing compelling evidence that bacterial-mediated interactions are critical in determining compatibility and disease dynamics in co-cultured seaweed systems. Overall, recognizing that IID symptoms can arise from multiple bacteria and depend on host genotype means that integrated control (combining resistant varieties, probiotic treatments, and strict farm management) is needed to mitigate this disease.

Interestingly, this study was able to disentangle the role of pathogenic bacteria and environmental factors in inducing IID. We showed that exposure to pathogenic bacteria isolated from an IID-infected cultivar can disrupt the microbiome and provoke IID syndrome among healthy plants under controlled and benign laboratory conditions.

In seaweed farms, incidence of IID is considered a complex pathobiotic syndrome (Ward et al. 2022), not caused by a single pathogen, but rather by a multifactorial interaction involving host susceptibility, opportunistic bacterial colonization, and environmental stress factors, the results of our study highlight the necessity of selecting disease-resistant genotypes and carefully monitoring microbial loads in farming environments to mitigate IID outbreaks. Future studies incorporating metagenomic and transcriptomic approaches are crucial to further elucidate the multifactorial etiology of IID and to develop effective biocontrol strategies, ensuring the sustainability of seaweed aquaculture.

Supplementary Information The online version contains supplementary material available at https://doi.org/10.1007/s10811-025-03776-7.

Authors' contribution HA Lestari: Conceptualization, Methodology, Investigation, Data Curation, Formal Analysis, Visualization, Writing-Original Draft, Writing- Review and Editing. F Izzuddin: Conceptualization, Resources, Writing- Review and Editing. W Purbiantoro: Conceptualization, Methodology, Investigation, Data Curation, Formal Analysis, Visualization, Writing- Review and Editing. YI Nababan: Methodology, Investigation, Writing- Review and Editing. ZA Siregar: Formal Analysis, Writing- Review and Editing. H Hikmaturrohmi,

ES Prasedya: Methodology, Resources, Writing- Review and Editing. MY Roleda: Supervision, Conceptualization, Methodology, Resources, Visualization, Writing- Original Draft, Writing- Review and Editing.

Funding Open access funding provided by Norwegian Institute of Bioeconomy Research The authors sincerely thank the Rumah Program, Research Organization for Earth Sciences and Maritime, National Research and Innovation Agency of Indonesia (BRIN), for financial support under Grant No. 3/III.4/HK/2025. Additional funding was provided by the *Riset dan Inovasi untuk Indonesia Maju (RIIM) Expedition Program,* Research Organization for Earth Sciences and Maritime, National Research and Innovation Agency of Indonesia (BRIN), under Grant Nos. B-1106/II/7.5/3/2024 and V-1680/III.4/HK.01.00/3/2024. MY Roleda received a 1-month Visiting Researcher Fellowship from BRIN.

Data availability The sequences of *Kappaphycus striatus* were deposited to GenBank and are available under accession numbers PX441407 (L1KS1) and PX441406 (L1M1). Bacterial sequences were deposited in GenBank with the accession numbers PX458025, PX458046, PX458079, and PX458080 for *V. chemaguriensis* (V1), *V. brasiliensis* (A8), *V. brasiliensis* (B2), *Cytobacillus* sp. (V2) bacteria, respectively.

Declarations

Conflicts of interests Michael Y. Roleda is an editorial board member of Journal of Applied Phycology and co-author of this article. He was excluded from editorial decision-making related to the acceptance of this article for publication in the journal. All other authors declare no conflicts of interests.

Open Access This article is licensed under a Creative Commons Attribution 4.0 International License, which permits use, sharing, adaptation, distribution and reproduction in any medium or format, as long as you give appropriate credit to the original author(s) and the source, provide a link to the Creative Commons licence, and indicate if changes were made. The images or other third party material in this article are included in the article's Creative Commons licence, unless indicated otherwise in a credit line to the material. If material is not included in the article's Creative Commons licence and your intended use is not permitted by statutory regulation or exceeds the permitted use, you will need to obtain permission directly from the copyright holder. To view a copy of this licence, visit http://creativecommons.org/licenses/by/4.0/.

References

Azizi A, Mohd Hanafi N, Basiran MN, Teo CH (2018) Evaluation of disease resistance and tolerance to elevated temperature stress of the selected tissue-cultured *Kappaphycus alvarezii* Doty 1985 under optimized laboratory conditions. 3 Biotech 8:321

Chang C-I, Lee C-F, Wu C-C, Cheng TC, Tsai J-M, Lin K-J (2011) A selective and differential medium for *Vibrio alginolyticus*. J Fish Dis 34:227–234

Dino A (2014) dunn.test: Dunn's Test of Multiple Comparisons Using Rank Sums. https://cran.r-project.org/web/packages/dunn.test/index.html. Accessed 12 October 2025

Dumilag RV, Crisostomo BA, Aguinaldo Z-ZA, Hinaloc LAR, Liao LM, Roa-Quiaoit HA, Dangan-Galon F, Zuccarello GC, Guillemin M-L, Brodie J, Cottier-Cook EJ, Roleda MY (2023) The diversity of eucheumatoid seaweed cultivars in the Philippines. Rev Fish Sci Aquacult 31:47–65

Gacura JRL, Hinaloc LAR, Oguira RN, Narvarte BCV, Aguilar RT, Mendoza EM, Projimo VZ, Roleda MY (2026) Exploiting the untapped wild resources: developing new diploid tetrasporophyte *Kappaphycus alvarezii* cultivars from sporelings of wild cystocarpic parental plants. Aquaculture 610:742916

Kambey CSB, Campbell I, Cottier-Cook EJ, Nor ARM, Kassim A, Sade A, Lim PE (2021) Seaweed aquaculture: a preliminary assessment of biosecurity measures for controlling the ice-ice syndrome and pest outbreaks of a *Kappaphycus* farm. J Appl Phycol 33:3179–3197

Kruskal WH, Wallis WA (1952) Use of ranks in one-criterion variance analysis. J Am Stat Assoc 47:583

Kus JV, Zaton K, Sarkar R, Cameron RK (2002) Age-related resistance in *Arabidopsis* is a developmentally regulated defense response to *Pseudomonas syringae*. Plant Cell 14:479–490

Largo DB, Fukami K, Nishijima T (1995) Occasional pathogenic bacteria promoting ice-ice disease in the carrageenan-producing red algae *Kappaphycus alvarezii* and *Eucheuma denticulatum* (Solieriaceae, Gigartinales, Rhodophyta). J Appl Phycol 7:545–554

Larkin MA, Blackshields G, Brown NP, Chenna R, McGettigan PA, McWilliam H, Valentin F, Wallace IM, Wilm A, Lopez R, Thompson JD, Gibson TJ, Higgins DG (2007) Clustal w and Clustal x version 2.0. Bioinformatics 23:2947–2948

Lim PE, Tan J, Phang SM, Nikmatullah A, Hong DD, Sunarpi H, Hurtado AQ (2014) Genetic diversity of *Kappaphycus* Doty and *Eucheuma* J. Agardh (Solieriaceae, Rhodophyta) in Southeast Asia. J Appl Phycol 26:1253–1272

Lin H-L, Lin C-C, Lin Y-J, Lin H-C, Shih C-M, Chen C-R, Huang R-N, Kuo T-C (2010) Revisiting with a relative-density calibration approach the determination of growth rates of microorganisms by use of optical density data from liquid cultures. Appl Environ Microbiol 76:1683–1685

Luhan MRJ, Avañcena SS, Mateo JP (2015) Effect of short-term immersion of *Kappaphycus alvarezii* (Doty) Doty in high nitrogen on the growth, nitrogen assimilation, carrageenan quality, and occurrence of "ice-ice" disease. J Appl Phycol 27:917–922

Ma M, Zhuang Y, Chang L, Xiao L, Lin Q, Qiu Q, Chen D, Egan S, Wang G (2023) Naturally occurring beneficial bacteria *Vibrio alginolyticus* X-2 protects seaweed from bleaching disease. MBio 14:e00065–23

Mendoza WG, Montaño NE, Ganzon-Fortes ET, Villanueva RD (2002) Chemical and gelling profile of ice-ice infected carrageenan from *Kappaphycus striatum* (Schmitz) Doty "sacol" strain (Solieriaceae, Gigartinales, Rhodophyta). J Appl Phycol 14:409–418

Muyong JS, Tahiluddin AB (2024) Interaction of nutrient enrichment and farming method on performance of the red seaweed *Kappaphycus alvarezii*. Aquat Bot 191:103743

Narvarte BCV, Nelson WA, Roleda MY (2020) Inorganic carbon utilization of tropical calcifying macroalgae and the impacts of intensive mariculture-derived coastal acidification on the physiological performance of the rhodolith *Sporolithon* sp. Environ Pollut 266:115344

Nguyen L-T, Schmidt HA, von Haeseler A, Minh BQ (2015) IQ-tree: a fast and effective stochastic algorithm for estimating maximum-likelihood phylogenies. Mol Biol Evol 32:268–274

Niedoba T, Surowiak A, Hassanzadeh A, Khoshdast H (2023) Evaluation of the effects of coal jigging by means of Kruskal-Wallis and Friedman tests. Energies 16:1600

Ogle DH, Doll JC, Wheeler AP, Dinno A (2015) FSA: Simple Fisheries Stock Assessment Methods. https://cran.uni-muenster.de/web/packages/FSA/FSA.pdf

Pang T, Liu J, Liu Q, Li H, Li J (2015) Observations on pests and diseases affecting a eucheumatoid farm in China. J Appl Phycol 27:1975–1984

Pang T, Wang F, Guo Q, Zhang M, Sun Y, Liu J (2025) *Vibrio alginolyticus* is the pathogen of "Baotou" disease causing serious damage to *Gracilariopsis lemaneiformis* cultivation in China. mBio 16:e03120–24

R Core Team (2025) R: A language and environment for statistical computing. R Foundation for Statistical Computing. R Foundation for Statistical Computing, Vienna, Austria. https://www.r-project.org/

Roleda MY, Hinaloc LAR, Capacio IT, Jao MCB, Crisostomo BA (2024) Reproductive biology and novel cultivar development of the eucheumatoid *Kappaphycus alvarezii*. In: Critchley aT, Hurtado AQ, Neish IC (eds) Tropical Phyconomy Coalition Development: Focus on Eucheumatoid Seaweeds. Developments in Applied Phycology 11. Springer, Cham, pp 41-45

Sherwani RAK, Shakeel H, Awan WB, Faheem M, Aslam M (2021) Analysis of COVID-19 data using neutrosophic Kruskal Wallis H test. BMC Med Res Methodol 21:215

Solis MJL, Draeger S, dela Cruz TEE (2010) Marine-derived fungi from *Kappaphycus alvarezii* and *K. striatum* as potential causative agents of ice-ice disease in farmed seaweeds. Bot Mar 53:587–594

Tahiluddin AB, Eldani-Tahiluddin (2024) Ice-ice disease in cultivated eucheumatoid seaweeds: The perspectives of farmers. Eur J Phycol 59: 423–435

Tahiluddin AB, Terzi E (2024) Ice-ice disease prevalence and intensity in eucheumatoid seaweed farms: seasonal variability and relationship with the physicochemical and meteorological parameters. Plants 13:2157

Vargha A, Delaney HD (1998) The Kruskal-Wallis test and stochastic homogeneity. J Educ Behav Stat 23:170–192

Ward GM, Kambey CSB, Faisan JP, Tan P, Daumich CC, Matoju I, Stentiford GD, Bass D, Lim P, Brodie J, Poong S (2022) Ice-ice disease: an environmentally and microbiologically driven syndrome in tropical seaweed aquaculture. Rev Aquacult 14:414–439

Publisher's Note Springer Nature remains neutral with regard to jurisdictional claims in published maps and institutional affiliations.